2018 21st International Conference on Intelligent Transportation Systems (ITSC)
Maui, Hawaii, USA, November 4-7, 2018

Robust Lane Keeping Control in Automated Vehicles: A Driver-in-the Loop Approach

Jagat Jyoti Rath*, Chouki Sentouh, *Member, IEEE* and Jean-Christophe Popieul

***Abstract*— The shared control between human driver and autonomous controller for vehicles has been evaluated over several driving conditions such as cruise control, lane keeping/ lane change assist, highway driving etc. Typically, these approaches synthesize controllers based on linear vehicle models integrated with visual cues based driver model. In this work, to consider the aspect of tire-friction non-linearity, Brush-Tire force model has been considered. Further, to address conflict between human driver and autonomous controller during typical maneuvers, a novel sharing parameter was introduced in the proposed robust sliding mode based control design. Subsequently, the proposed shared control technique is validated thru numerical simulations over the Satory test track, with lateral wind force and road curvature considered as disturbance. Discussions on influence of varying road-friction conditions and sharing parameter proposed is also presented.**

I. Introduction

The incorporation of advanced driver assistance systems (ADAS) [1] such as lane keeping assist [2], [3], collision avoidance [4], automated trajectory planning [5], adaptive cruise control [6], etc. in modern automobiles have reduced traffic accidents and made life easier for the human driver. With semi or fully autonomous control features, the ADAS system overtake the control of the vehicle from the human driver for some typical driving scenarios. A better interaction of the intelligent ADAS with the human driver while navigating these driving scenarios is paramount in ensuring driving performance [4]. In the aspect of shared control, the control objective is that the human-machine interaction should occur such that transition of control from the human to the machine and vice-versa achieves a typical driving task. Recent researches [2], [7]–[9] have explored the avenue of shared control between human driver and automated system to improve the driving performance.

In [7], [10], the use of haptic feedback from the steering wheel was considered to analyze the shared control performance. Based on varying degrees of assistance provided, a subjective assessment of the control performance was conducted. The influence of cognitive driver parameters such as fatigue, drowsiness [2], [3], intention [11] etc., along with other factors such as road geometry, driver behavior, trust etc. were evaluated as some of the factors contributing to the shared control performance. Subsequently in [2]–[4], [8], [9], [12], [13] various driver-in-the-loop shared control approaches were explored to account for driver characteristics in the control design.

In [8], based on a closed loop driver-vehicle model a shared control approach employing was proposed for lane keeping. The shared control performance based on nuero-muscular driver model integrated with linear vehicle-road model was evaluated for consistency, resistance and contradictions between the driver and automated system. Similarly in [12], a haptic shared control between driver and e-copilot considered the use of driver torque as haptic feedback to design T-S fuzzy controllers for lane keeping. In [9], for varying driver steering characteristics such as delays, preview time etc. a driver-in-the-loop gain-scheduling H-∞ robust shared controller was proposed. Similarly in [13], a novel driver model employing a motion stabilizer and real time velocity planner was proposed to design an integrated speed -steering controller. Other shared control approaches such as [3], [14] designed intelligent e-copilot based shared control approaches which accounted for driver attributes such as driver torque, driver state, workload etc.

Considering the human-machine interaction between ADAS systems and the human driver, contradictions between driver and automated system while navigating some typical maneuvers is inevitable. In [7], [10] the aspect of conflict between human driver and the autonomous driving system was also discussed. Further, in [15] the importance of taking into consideration driver reactions for the design of road departure prevention systems was addressed. In [2], [3], by the design of shared control dependent on driver attributes, the issue of conflict between the driver and automated system was addressed for variable longitudinal speeds. The management of conflict was not explicitly addressed in [9], [13], [14]. Further, the previous works proposed approaches based on the linearized vehicle model that did not take into consideration the nonlinear tire-friction behavior.

To account for nonlinearities in the vehicle model and conflict aspect between driver-autonomous driving system, a robust sliding mode [16], [17] based shared control approach is proposed in this work. The Brush-tire friction model [18] is employed to develop the nonlinear vehicle model corresponding to steering action under variable longitudinal speeds. The nonlinear vehicle-road model was then integrated with the driver model [2], to formulate a driver in-the-loop model. Integrating the driver attributes of state and variations in driver torque, a weighted assist control parameter was designed based our previous work [2]. To

This work has been done in the framework of the the CoCoVeA research program (ANR-13-TDMO-0005), funded by the National Research Agency. This work was also sponsored by the Regional Delegation for Research and Technology, the Ministry of Higher Education and Research, the French National Center for Scientific Research.

Jagat Jyoti Rath, Chouki Sentouh, and Jean-Christophe Popieul are with LAMIH-UMR CNRS 8201, University of Valenciennes, France. Email: jagatjyoti.rath@gmail.com, Chouki.Sentouh@uphf.fr, Jean-Christophe.Popieul@uphf.fr

account for the conflict, a fictional state with a sharing parameter was then introduced into the design of a sliding surface. Subsequently to minimize the lane following errors i.e. lateral deviation and heading error along with conflict and to increase driver comfort, a robust sliding mode controller based on super-twisting approach (STA) [16], [17] was proposed. The closed loop stability analysis of the proposed state feedback controller when subject to disturbances such as wind force and road curvature was established similar to [16], [17]. The performance of the shared control approach was validated over simulations for adaptive driving, conflict reduction over the Satory test track and disturbance rejection w.r.t lateral wind forces.

II. Problem Formulation

In this section, the nonlinear interaction between the vehicle-road is modeled using the Brush-Tire model. Further, a driver-in-the-loop architecture is developed and subsequently the control objectives i.e. lane keeping and conflict between human driver and autonomous driving system are established for a vehicle with parameters given in Table. I.

TABLE I
Driver-Vehicle Parameters

Parameter	Value
Mass (M)	1500 Kg
Yaw Inertia (I_z)	2250 Kgm^2
Steer Inertia (J_s)	0.05 Kgm^2
Distance to front (l_f)	1 m
Distance to rear (l_r)	1.5 m
Front tire stiffness (C_{pf})	47135 N/rad
Rear tire stiffness (C_{pr})	56636 N/rad
Steer damping (B_u)	0.25
Steer gear ratio (R_s)	21
Steer Stiffness (K_s)	1.3232
Compensatory gain (K_c)	6.15
Anticipatory gain (K_a)	15.70
Preview time (T_p)	0.8 s
Look ahead distance (l_p)	5 m
Time to tangent (τ_a)	1.05 s
Tire trail (t_p)	0.13 m

A. Vehicle-Road-Driver Modeling

The governing dynamics for the lateral motion of a vehicle comprises of transnational and rotational components. Considering the tire-road based friction excitation and the steering dynamics to represent driver feeling, it can be written: [1], [18]

$$\dot{\beta} = \frac{1}{Mv_x}\left[F_{yr} + F_{yf}cos(\delta_f) - Mv_x\dot{\psi}_p + F_w\right] \quad (1)$$

$$\dot{r} = \frac{1}{I_z}\left[l_f F_{yf}cos(\delta_f) - l_r F_{yr} + M_w\right] \quad (2)$$

$$\ddot{\delta}_d = \frac{1}{J_s}\left[T_d + T_c - T_s - B_u\dot{\delta}_d - K_u\delta_d\right] \quad (3)$$

where β is the side slip, r is the yaw rate, the longitudinal velocity is v_x, δ_d is the driver steering angle, driver and autonomous controller torques are T_d and T_c respectively, T_s is the self-align torque, and F_w is the lateral wind force. The steering angle of the wheel δ_f is related to the driver steering angle as $\delta_f = \lambda\delta_d$, where $\lambda = 1/Rs$. The interaction between tires and ground is modeled using the nonlinear Brush-Tire model [18] and given as:

$$F_{yi} = \begin{cases} 3\zeta_i\left[1 - |\theta_{yi}e_{yi}| + \frac{1}{3}(\theta_{yi}e_{yi})^2\right]; \forall\alpha_i \le \alpha_{sli} \\ \mu F_z sign(\alpha_i) \quad ; \forall\alpha_i > \alpha_{sli} \end{cases}$$

with, $\zeta_i = \mu F_z\theta_{yi}e_{yi}$, $\alpha_{sli} = tan^{-1}(\frac{1}{\theta_{yi}})$, $\theta_{yi} = \frac{2C_{pi}l_p^2}{3\mu F_z}$, $e_{yi} = tan(\alpha_i)$, $i = f, r$ denotes the front and rear of the vehicle and C_{pi} is the tire stiffness. Based on the friction of the road condition, the relationship between the vehicle side-slip and friction force can be shown as It can be deduced

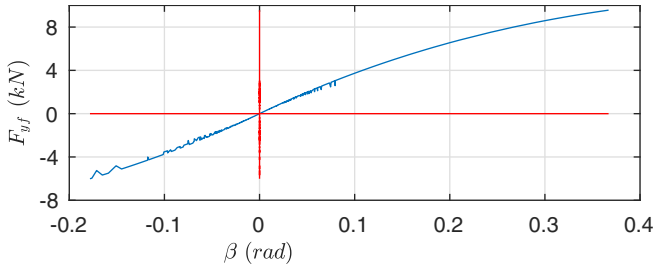

Fig. 1. The relationship between lateral tire friction- side slip angle for variable friction scenarios.

from Fig. 1 that the relationship is nonlinear in nature. Under low slip conditions, the relationship is linear. For the font wheel steering drive considered in this work and under small angle assumption, the slip angles can be then given as:

$$\begin{cases} \alpha_f &= \delta_f - \frac{\beta v_x + l_f r}{v_x} \\ \alpha_r &= \frac{\beta v_x - l_r r}{v_x} \end{cases}$$

where f, r denote the front and rear slip angles. The wheel steer angle is given as a function of the driver steer angle i.e. $\delta_f = \lambda\delta_d$, where $\lambda = 1/Rs$. The resistance to the vehicle steering i.e. the self-align torque can be expressed as a function of pneumatic tire trail t_p and given as $T_s = \lambda K_p t_p F_{yf}$, with K_p denoting the level of assistance from the active steering system. For lane keeping, two supplementary variables i.e. lane deviation error (y_l) and heading error (Ψ_l) are then defined similar to [2], [12]

$$\dot{y}_l = \beta v_x + l_p r + \Psi_l v_x; \quad \dot{\Psi}_l = r - \rho_r v_x \quad (4)$$

where where the desired heading is given as $\Psi_c = \rho_r v_x$ with ρ_r representing the road curvature. To develop a driver-in-the-loop model, the model of human driver based on visual clues similar to [2] has been developed as:

$$T_d = K_c\theta_n + K_a\theta_f \quad (5)$$

where θ_n, θ_f denote the near and far visual angles. Based on the preview time T_p, the driver compensates his near visual angle. Similarly, he far visual angle information can be obtained from the predicted road curvature based on the far look ahead distance ($L_f = \tau_a v_x$). The near and far visual angles can be obtained as: [2], [3]

$$\theta_n = \frac{y_l}{v_x T_p} + \Psi_l; \quad \theta_f = L_f \frac{r}{v_x} + L_f^2 \frac{\dot{r}}{v_x^2} \tag{6}$$

with T_p denoting the preview time. Integrating the nonlinear vehicle dynamics (1)-(3) with the lane keeping performance parameters (4) and the driver torque model (5), a closed driver in the loop nonlinear system can be formulated as

$$\dot{x} = f(x,u) + g(x,u)U + \Delta\theta \tag{7}$$

where the states are $x = \begin{bmatrix}\beta & \psi & y_l & \Psi_l & \delta_d & \dot{\delta}_d\end{bmatrix}^T$, $f(x,u)$ represents the dynamics of the states detailed earlier, U is the assist control T_c to be designed and θ represents the disturbances affecting the dynamics i.e. road curvature (ρ_r), wind force (F_w) and wind moment (M_w).

B. Shared Control: Human-Machine Interaction

The relationship between the driver and autonomous driving system depends on various parameters such as driver torque, driver state, driver intention, behavior, skills, environmental disturbances, effect of driving conditions etc. In this work, considering the effects of driver torque and driver state a nonlinear relationship that represents driver activity function (Γ) was considered as [2], [3]

$$\Gamma = 1 - e^{-(e_1 T_{dN})^{e_2} DS^{e_3}} \tag{8}$$

with $e_1 = 2, e_2 = e_3 = 3$, $0 \leq DS \leq 1$, $T_{dN} = |T_d / T_{d_{max}}|$. The parameters e_2 and e_3 represent the involvement of the driver torque and driver state on the driver activity function. The driver state is normalized as $0 \leq DS \leq 1$, where 0 represents a drowsy driver and 1 represents a watchful driver. Thus if the value of DS is low, then a higher level of assistance is required and vice-versa. For lower driver torques indicating under-load conditions, low assistance is required to carry out a driving task. For high driver torques i.e. overload conditions, higher assistance is required. This relationship between driver work-load and level of assistance required can be shown as a 'U" shaped function as shown in Fig. 2 [2]. Based on the above shown assistance curve and the driver activity (8), a nonlinear function can be modeled as

$$f(\Gamma) = \frac{1}{1 + |\frac{\Gamma - p_3}{p_1}|^{2p_2}} + f_{min} \tag{9}$$

where $p_1 = 0.355, p_2 = -2$ and $p_3 = 0.5$. The minimum value of $f(\Gamma)$ is fixed at $f_{min} = 0.2$ based on tests conducted on vehicle simulator. Subsequently, the relationship between Γ and $f(\Gamma)$ is shown in Fig. 2. Integrating the developed driver activity function into the controller design, the autonomous torque can be then modulated as

$$T_c = f(\Gamma)\ U \tag{10}$$

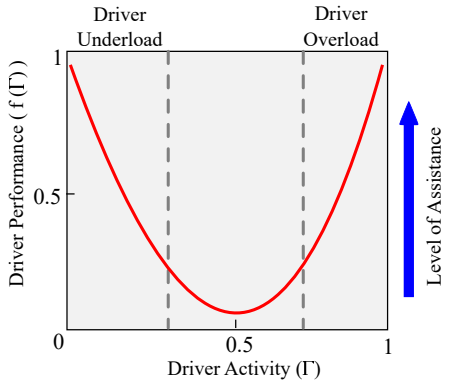

Fig. 2. The relation between driver activity and driver performance i.e. Γ and $f(\Gamma)$

where U is the nonlinear feedback control to be designed. The control objectives for the driver-in-the loop system can be then expressed as:

- *Minimize the lane deviation errors* i.e. Ψ_l and y_l for variable friction conditions.
- *Reduce conflict between driver and automated system.*

III. Robust Controller for Lane Keeping

In this section, a robust controller employing the higher order sliding mode (HOSM) based STA approach is now proposed to achieve the control objectives. For the considered driver-in-the-loop design, it should be noted that in the scenario when $T_d = 0$, the vehicle is controlled entirely by the autonomous system. Similarly, when $T_c = 0$, there is only human driver present and no autonomous controller. In the event of cooperative driving, both T_d and T_c have non-zero values. The parameters which characterize lane keeping performance are the lateral deviation error and heading error i.e. y_l and Ψ_l respectively. Similarly the increase in driver comfort can be quantified by the decrease in lateral acceleration or the rate of driver steering angle i.e. $\dot{\delta}_d$. The conflict between human driver and autonomous controller is measured in this work as the product of torques i.e. Conflict = $T_d T_c$. The product of these torques signify the nature of assistance provided to the driver i.e. if the product of the torques is positive then its and assisting torque [2], [3]. However if $T_d T_c < 0$ i.e. the product is negative then the torques generated by the driver and system are conflicting [2], [3]. This condition arises in scenarios such curve negotiation, disturbance rejection etc and the conflict in such scenario needs to be minimized. To design the effective assist control T_c which accomplishes the control objectives, the following error surface is thus considered

$$e = k_1(l_s \Psi_l + y_l) + k_2 \dot{\delta}_d + \lambda k_3 x_{cf} \tag{11}$$

where k_1, k_2, k_3 are the control gains to be designed and x_{cf} is a fictional state which represents the conflict between driver and automated system. The dynamics of this state is given as

$$\dot{x}_{cf} = T_d T_c \tag{12}$$

The control objective is thus to force the error surface e to zero in the presence of external disturbances (i.e. ρ_r, F_w, M_w) by the design of a nonlinear robust control T_c. To stabilize the error dynamics by the design of a state feedback control, the following theorem is proposed.

Theorem 1: For the nonlinear integrated driver-vehicle system with the error surface e and the gains $k_1...k_4 > 0$, the following control law is proposed.

$$U = \frac{1}{\tau}\left[-\Omega(x) + \zeta(e)\right] \tag{13}$$

where $\tau = (\frac{k_3 + k_4 \lambda T_d}{J_s})$, $\Omega(x)$ is a function of states to be defined later and $\zeta(e)$ is the robust HOSM term based on modified STA [16], [17] given as

$$\zeta(e) = -\gamma_1 \phi_1(e) - \gamma_2 \int_0^t \phi_2 \, dt \tag{14}$$

with $\phi_1(e) = e + \gamma_3 |e|^{\frac{1}{2}} sign(e)$, $\phi_2(e) = e + 0.5\gamma_3^2 sign(e) + 1.5\gamma_3 |e|^{\frac{1}{2}} sign(e)$ and $\gamma_1, \gamma_2, \gamma_3 > 0$ are the positive gains to be designed. Employing the above nonlinear control law U with the robust HOSM term $\zeta(e)$, the error surface and its derivative converges to zero in finite time, $e = \dot{e} = 0$.

Proof: From (11), the dynamics of the error surface can be then expressed as

$$\dot{e} = k_1(l_s \dot{\Psi}_l + \dot{y}_l) + k_2(l_s \ddot{\Psi}_l + \ddot{y}_l) + k_3 \dddot{\delta}_d + \kappa_4 \lambda T_c T_d \tag{15}$$

It can be hence seen, that the error dynamics are a function of vehicle dynamics and the disturbances i.e. road curvature and wind disturbance. Considering (15) by substituting for vehicle dynamics, we can write

$$\dot{e} \;=\; \Omega + \left[\frac{k_3}{J_s} + k_4 \lambda T_d\right] f(\Gamma) U + \Theta$$

where $\Omega = k_1 f_1(x) + k_2 f_2(x) + k_3 f_3(x)$. The functions $f_1(x), f_2(x)$ and $f_3(x)$ are given as

$$f_1(x) \;=\; 2l_s r + v_x(\beta + \Psi_l), \;\; f_2(x) = 2l_s \dot{r} + v_x(\dot{\beta} + r)$$
$$f_3(x) \;=\; \frac{1}{J_s}(T_d - T_s - B_u \dot{\delta}_d)$$

The disturbance term Θ is given as $\Theta = -k_2 v_x \rho_r + k_2 v_x (M_w/I_z) + K_2(F_w/M) - (k_1 \rho_r + k_2 \dot{\rho}_r) l_s v_x$. Employing the control law (13), the error dynamics can be expressed as

$$\dot{e} = \zeta(e) + \Theta \tag{16}$$

Under the assumptions that for the considered vehicular system, the disturbances and their rate of change are bounded, it can be shown that $|\dot{\Theta}| < \delta$. The convergence of the error dynamics in finite time i.e. $e = \dot{e} = 0$ can be then established by the design of the gains γ_1, γ_2 and γ_3 similar to [16], [17]. For detailed proof refer [16], [17]. ■

IV. Results & Discussion

In this section the simulation results evaluated on MATLAB/ Simulink platform are presented validating the proposed nonlinear controller for the vehicle parameters shown in Table. I. The performance of the proposed nonlinear controller has been analyzed as the vehicle traversed over the Satory test track [2] shown in Fig. 3. The vehicle's

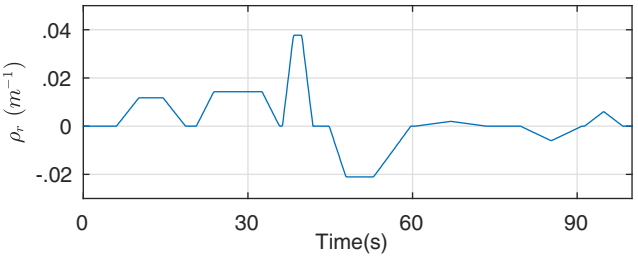

Fig. 3. The Satory test track with variable road curvatures.

performance was evaluated as the vehicle traversed at fixed longitudinal speed of $v_x = 14m/s$. For the driver-vehicle system considered, the disturbances F_w, M_w and ρ_r are bounded and the design gains were selected as $k_1 = 8$, $k_2 = 7$, $k_3 = 0.5$, $\kappa_4 = 0.05$, $\gamma_1 = 1.5$, $\gamma_2 = 8$ and $\gamma_3 = 1.5$ such based on the bounds of the perturbations to ensure convergence of the sliding surface [16], [17]. For the above operating conditions the controlled system states must be bound as $-0.55rad \leq \psi \leq 0.55rad$, $-0.3rad \leq \dot{\delta}_f \leq 0.3rad$, $-1.75m \leq y_l \leq 1.75m$ and $-0.15rad \leq \Psi_l \leq 0.15rad$. For the proposed shared control, the driver anticipatory and compensatory gains were chosen as $K_a = 15.70$ and $K_c = 6.8$. To reflect the Human-Machine Interaction (HMI) and ensure efficient control, it was considered that the state of the driver varies through the course. Subsequently, during a high curve the driver was considered more watchful than during a lower curve. To ensure different sharing levels, the driver state was varied such that for $t \in [0, 20]s$ the $DS = 0.45$, $t \in [20, 35]$ s the $DS = 0.8$ (highly active), $t \in [35, 45]$ s the $DS = 0.3$, $t \in [45, 75]$ s the $DS = 0.55$ and from $t \in [75, 100]$ s the $DS = 0$ (i.e. autonomous controller). Further the maximum driver torque level was fixed at $T_{d_{max}} = 6Nm$. For the above considered Satory test track and operating scenarios, the lane keeping performance of the vehicle based on the proposed shared control approach was evaluated.

A. Lane keeping: Variable Road Friction

Employing the Brush-tire friction model, nonlinear friction behavior was considered in this work. To evaluate the performance of the controller, the friction coefficient μ was varied as $\mu = 0.5$ during $t \in (0, 25)s$, $\mu = 1$ during $t \in (25, 45)s$, $\mu = 0.7$ during $t \in (45, 75)s$ and $\mu = 0.4$ during $t \in (75, 100)s$. The lane keeping control of the vehicle under such variable friction conditions can be represented by the lateral deviation and heading errors as shown in Fig. 4. During the entire course of the trajectory, the root mean square error (RMSE) of these entities was computed. Consequently, the RMSE of lateral deviation i.e. $y_{l_{RMS}} = 0.1881$ and the RMSE of heading was found as $\Psi_{l_{RMS}} = 0.0284$. It can also be deduced from Fig. 4, that during the duration $t \in [25, 45]s$ the magnitudes of y_l and Ψ_l are comparatively higher. This corresponds to the high road curvature region as can be seen from Fig. 3.

The corresponding lateral acceleration, yaw rate and steering states for the vehicle are shown in Fig. 5. As shown in Fig. 5 (a), the lateral acceleration of the controller vehicle is bounded within ranges of $|a_y| \pm 4m/s^2$. Similarly the yaw rate, steering angle and steering rate are also bounded with the operating limits discussed earlier. For the above

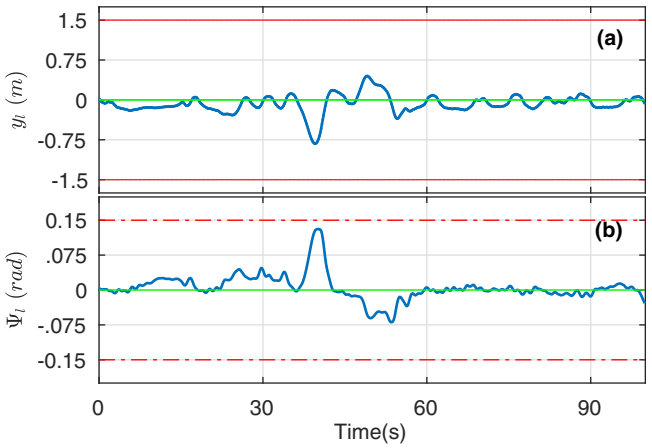

Fig. 4. The lane keeping performance by minimization of (a) lateral deviation (b) heading error.

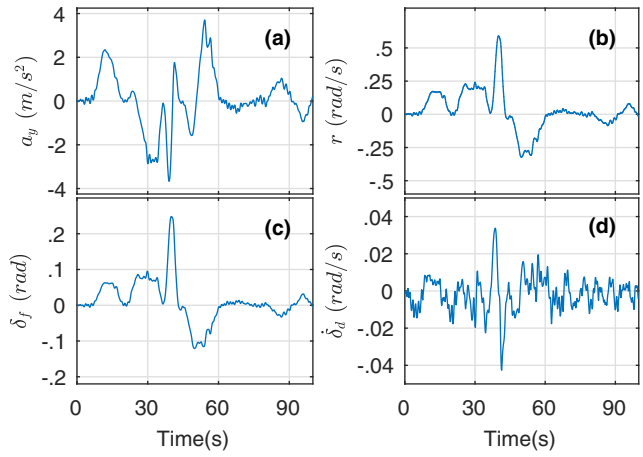

Fig. 5. The (a) lateral acceleration (b) yaw rate (c) steering angle (d) steering angle rate for the vehicle.

driving conditions, the interaction between the driver and the autonomous driving system is shown in Fig. 6 (a). It can be seen from Fig. 6 (a), that corresponding to the road curvatures, driver state and road friction conditions, the driver activity varies over the entire track. Typically, on average during $t \in [20, 60]s$ the activity is high as the driver navigates high curves with assistance from the autonomous driving system. Thus the level of sharing varies depending on driver activity. The corresponding torques generated by the human driver and the assist system are shown in Fig. 6 (b). It can be seen that both the torques are within the operating limits established before. Further, in accordance with the HMI behavior the torques are generated by driver and the autonomous system.

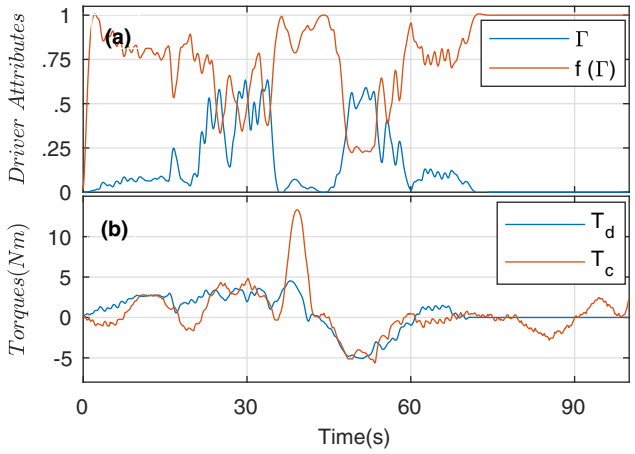

Fig. 6. The human-machine interaction (a) driver activity and performance (b) driver and assist torques.

To further analyze the significance of friction, fixed friction conditions over the entire track were considered. Further by comparing with a linear friction model the graphical illustration of side slip angle is shown in Fig. 7. It can be seen from Fig.7, that for high fixed friction values, the proposed shared controller has low side slip values for both the linear and non-linear friction models. However, as the friction magnitude decreases below $\mu = 0.9$, the side slip angle increases significantly and ultimately leads to tire force saturation. This significantly occurs during the phase $t \in [35, 50]s$ where the vehicle navigates a high curve. However, employing the nonlinear friction model variable friction conditions can be analyzed. To show efficient lane keeping performance, the computed RMSE for lateral deviation and heading for various conditions is shown in Table. II. It can be concluded from the

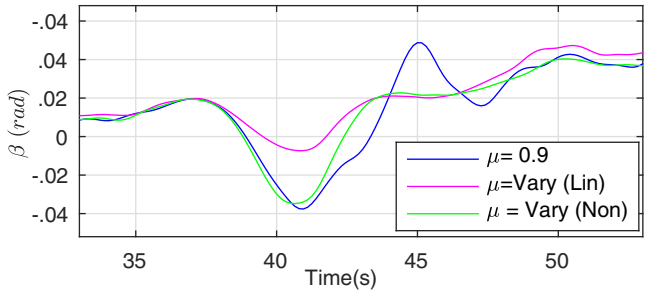

Fig. 7. The variable tire slip at velocity of $v_x = 14m/s$ for $\mu = 0.9$, Linear Friction Model with variable friction, Proposed Nonlinear design

presented results in Table. II that the proposed shared control approach provides an efficient lane keeping performance for variable friction and high fixed friction conditions.

B. Conflict management between the human-autonomous driving system

In this paper, a novel shared control parameter κ_4 was introduced to moderate the conflict between the human driver and the autonomous driving system. To show the effect of this parameter, the product of the torques as discussed in

TABLE II

LANE KEEPING PERFORMANCE AT $v_x = 14m/s$

μ	$y_{l_{RMS}}$	$\Psi y_{l_{RMS}}$
$\mu = 1$	0.3292	0.0356
$\mu = 0.9$	0.6369	0.0441
$\mu = 0.8$	Saturated	Saturated
$\mu = Vary$ (Linear)	0.2663	0.0324
$\mu = Vary$ (Nonlinear)	0.1881	0.0284

Section III, has been considered. The sharing parameter is designed such that conflict i.e. $T_d T_c < -\eta$, where $\eta > 0$ is any positive parameter. In this work, considering $\eta = 3$, the graphical illustration of conflict for different values of the parameter k_4 is shown in Fig. 8. It can be seen from

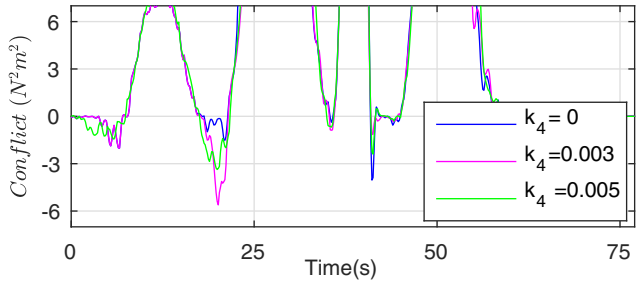

Fig. 8. A representation of conflict as the product of driver and autonomous torque for different values of sharing parameter k_4.

Fig. 8, that with the increasing values of the parameter k_4 the magnitude of conflict decreases in general. Typically during high curve regions such as during $t \in [40, 45]$ s, the increase in value of k_4 decreases the magnitude of conflict between the driver and the autonomous driving system. However for higher values of k_4, during low curve regions i.e. $t \in [15, 20]$ s there is an increase in the conflict status. Thus, the choice of the conflict parameter is subjective to the driving conditions. Further, the introduction of the sharing parameter k_4 influences how the torques interact with each other. This in turn influences the lane keeping performance of the vehicle and steers the vehicle off the lane for very high values. It can be concluded that the sharing parameter k_4 can be designed such that objectives of lane keeping are not compromised while minimizing conflict for typical scenarios such as obstacle avoidance, lane change etc. where conflict appears significantly.

V. CONCLUSION

In this work a robust shared control approach between human driver and automated system was evaluated over various driving scenarios. To account for tire force nonlinearities, the Brush-tire force model was considered in the development of the integrated driver-vehicle model. The proposed control approach also accounted for the conflict between human and machine, by incorporating a sharing parameter into the design. Further adaptive driving results over the Satory test track were presented highlighting control performance during cognitive under-load, overload and conflict scenarios.

REFERENCES

[1] R. Rajamani, "Vehicle Dynamics and Control," *Boston, MA: Springer, US*, 2012.

[2] A. T. Nguyen, C. Sentouh and J. C. Popieul,"Driver-Automation Cooperative Approach for Shared Steering Control under Multiple System Constraints: Design and Experiments," *IEEE Transactions on Industrial Electronics*, vol. 64, no. 5, pp. 3819–3830, 2017.

[3] C. Senotuh, A. T. Nguyen, M. A. Benloucif and J. C. Popieul , "Driver-automation cooperation oriented approach for shared control of lane keeping assist systems," *IEEE Transactions on Control Systems Technology*, 2018, DOI:10.1109/TCST.2018.284221.

[4] S. C. Schnelle, J. Wang, H. J. Su and R. Jagacinski, "A Personalizable Driver Steering Model Capable of Predicting Driver Behaviors in Vehicle Collision Avoidance Maneuvers," *IEEE Transactions on Human-Machine Systems*, vol. 47, no. 5, pp. 625–635, 2017.

[5] J. Nilsson, M. Brannstrom, J. Fredriksson and E. Coelingh,"Longitudinal and Lateral Control for Automated Yielding Maneuvers, *IEEE Transactions on Intelligent Transportation Systems*, vol. 17, no. 5, pp. 1404–1414, 2016.

[6] A. F. Idriz, A. S. A. Rachman and S. Baldi,"Integration of autosteering with adaptive cruise control for improved cornering behaviour," *IET Intelligent Transport Systems*, vol. 11, no. 10, pp. 667-675, 2017.

[7] F. Mars, M. Deroo and J. M. Hoc, "Analysis of Human-Machine Cooperation When Driving with Different Degrees of of Haptic Shared Control," *IEEE Transactions on Haptics*, vol. 7, no. 3, pp. 324-333, 2014.

[8] L. Saleh, P. Chevrel, F. Claveau, J. F. Lafay and F. Mars,"Shared Steering Control Between a Driver and an Automation: Stability in the Presence of Driver Behavior Uncertainty," *IEEE Transactions on Intelligent Transportation Systems*, vol. 14, no. 2, pp. 974–983, 2013.

[9] J. Wang, G. Zhang, R. Wang, S. C. Schenelle and J. Wang, "A Gain-Scheduling Driver Assistance Trajectory Following an Algorithm Considering Different Driver Steering Characteristics," *IEEE Transactions on Intelligent Transportation Systems*, DOI: 10.1109/TITS.2016.2598792, 2016.

[10] R. Boink, M. M. Van Paassen, M. Mulder and A. D. Abbink, "Understanding and Reducing Conflicts between Driver and Haptic Shared Control," *In Proc. of IEEE International Conference on Systems, Man, and Cybernetics*, pp. 1510-1515, 2014.

[11] A. Mukhtar, L. Xia and T. B. Tang, "Vehicle Detection Techniques for Collision Avoidance Systems: A Review," *IEEE Transactions on Intelligent Transportation Systems*, DOI: 10.1109/TITS.2015.2409109, 2015.

[12] B. Soulami, C. Sentouh, J. C. Popieul and S. Debernard, "Automation-driver cooperative driving in presence of undetected obstacles", *Control Engineering Practice*, vol. 24, pp. 106–119, 2014.

[13] Y. Koh, H. Her, K. Yi and K. Kim, "Integrated Speed and Steering Control DriverModel for VehicleDriver Closed-Loop Simulation," *IEEE Transactions on Vehicular Technology*, vol. 65, no. 6, pp. 4401–4411, 2016.

[14] N. A. Oufroukh and S. Mammar, "Integrated Driver Co-pilote Approach for Vehicle Lateral Control", *In Proc. of IEEE Intelligent Vehicles Symposium*, pp. 1163-1168, 2014.

[15] D. I. Katzourakis, J. C. F. de Winter, M. Alirezaei, M. Corno and R. Happee, "Road Departure Prevention in an Emergency Obstacle Avoidance Situation," *IEEE Transactions on Systems, Man and Cybernetics: Systems*, vol. 44, no. 5, pp. 621–629, 2014.

[16] J. J. Rath, K. C. Veluvolu and M. Defoort, "Simultaneous Estimation of Road Profile and Tire Road Friction for Automotive Vehicle", *IEEE Transactions on Vehicular Technology*, vol. 64, no. 10, pp. 4461–4471, 2015.

[17] J. A. Moreno and M. Osorio, "Strict Lyapunov functions for the super-twisting algorithm," *IEEE Transactions on Automatic Control*, vol. 57, no. 4, pp. 1035–1040, 2012.

[18] C. Ahn, H. Peng and H. E. Tseng, "Robust Estimation of Road Frictional Coefficient", *IEEE Transactions on Control Systems Technology*, vol. 21, no. 1, pp. 1–12, 2013.